Exploring the electronic structure and speciation of aqueous and colloidal Pu with high energy resolution XANES and computations†

Tonya Vitova, * Ivan Pidchenko, David Fellhauer, Tim Pruessmann, Sebastian Bahl, Kathy Dardenne, Tadahiro Yokosawa, Bernd Schimmelpfennig, Marcus Altmaier, Melissa Denecke, Jörg Rothe and Horst Geckeis

Pu L_3 HR-XANES and FEFF9 computations provide evidence for band-like 6d states in colloidal Pu contrasting to narrow 6d states in molecular Pu(IV). Pu L_3 HR-XANES is valuable for bond length estimation in plutonyl, whereas Pu M_5 HR-XANES is an advanced tool for analysing Pu redox states and 5f unoccupied density of states.

Plutonium (Pu) is one of the elements with an exceptionally complex chemistry and the ability to coexist in four different oxidation states under environmentally relevant conditions, each showing unique geochemical properties.[1,2] It is well known that Pu(IV) has a high tendency towards hydrolysis, polymerization and subsequent colloid formation depending on pH and Pu concentration. Even though such species have a significant impact on Pu solubility and mobility in the environment, their structure is still not well understood and remains controversial. There is evidence that Pu colloids contain oxidic and more amorphous domains and also different Pu redox states, *inter alia* Pu(V), depending on Eh and pH.[1–3]

Previous laser induced breakdown detection (LIBD) investigations show formation of colloids in aqueous Pu(IV) solutions at pH 1.8.[4,5] Extended X-ray absorption fine structure (EXAFS) analyses indicate a ripening of the colloids into crystalline nanoparticles with fluorite-like structure. Reduction of the most intense absorption peak (white line, WL) amplitude for aged colloids compared to that of Pu(IV) aquo species in the Pu L_3 absorption edge X-ray absorption near edge structure (XANES) (Pu L_3 XANES) is proposed to be due to transfer from narrow well defined to band-like (condensation) Pu 6d states of the Pu(IV) species upon transitioning from molecular to solid state;[4,5] However, no quantum chemical computations have been performed to verify this notion. Rothe *et al.* ruled out increased structural disorder and higher electronic density in the 6d states as being responsible for such spectral changes.[4] However, it cannot be completely excluded that minor amounts of Pu in redox states different from IV may also lead to WL reduction. For example, evidence for Pu(V) stabilized in Pu(IV) colloids is concluded from nano-electrospray time-of-flight mass-spectrometry (ESI-TOF-MS).[5]

Herein, we present a Pu L_3 and M_5 X-ray absorption fine structure (XAFS = XANES + EXAFS) and high energy resolution XANES (HR-XANES)[6–8] investigation of aqueous solutions of plutonium in a series of oxidation states (Pu(III)aq–Pu(VI)aq), aged Pu(IV) colloids (Pu(IV)col) and crystalline PuO_2; only L_3 and M_5 HR-XANES data are discussed for the Pu(V)aq and PuO_2, respectively. Pu L_3 and $M_{4,5}$ HR-XANES directly probe the lowest unoccupied Pu 6d (L_3) and 5f (M_5) states.[7,8] Experimental results are substantiated by *ab initio* quantum chemical calculations of Pu L_3 HR-XANES and density of states (DOS) applying the FEFF9.5 code (*cf.* ESI†). The sensitivity of Pu M_5 HR-XANES to mixtures of Pu oxidation states in solutions is demonstrated. We discuss potential evidence for the presence of Pu oxidation states higher than Pu(IV) in eigen-colloids and condensation effects on the 6d states going from molecular to colloidal Pu(IV) species.

It is essential to validate that the Pu oxidation states are not affected by redox reactions, synchrotron radiation and/or handling and transportation. The Vis-NIR spectra of the four electrochemically prepared Pu(III)aq–Pu(VI)aq solutions and the Pu(IV)col sample were measured before and after the synchrotron experiments (with the exception of Pu(IV)col sample after the Pu M_5 HR-XANES) and no large changes in oxidation states are detected (Fig. S1, ESI†). The spectra for Pu(IV)aq demonstrate the presence of 9% (L_3 data) and 6% (M_5 data) Pu(VI), but only a 2% oxidation state variations before and after the synchrotron experiments. 7% of the initial Pu(V)aq is observed to disproportionate to [6% Pu(IV)col + 1% Pu(VI)aq].

The EXAFS analyses for the aqueous Pu species reveal coordination of Pu(III)aq to 10.5(8) O at 2.48(1) Å and 11.2(5) O at 2.34(1) Å for Pu(IV)aq (Table S2, ESI†). The Pu(V)aq and Pu(VI)aq Fourier transformed-EXAFS (FT-EXAFS) spectra exhibit two intense peaks (Fig. S6, ESI†). The peak at shorter Pu–O

Institute for Nuclear Waste Disposal (INE), Karlsruhe Institute of Technology, P.O. 3640, D 76021 Karlsruhe, Germany. E mail: Tonya.Vitova@kit.edu

† Electronic supplementary information (ESI) available: Preparation of the samples, experimental (XAS, Vis NIR, TEM) and computational (FEFF9.5, TURBO MOLE) details. See DOI: 10.1039/c8cc06889e

interatomic distance corresponds to the *trans*-dioxo bond typical for PuO_2^{1+}/PuO_2^{2+} (plutonyl); the second peak corresponds to distances for the equatorial O atoms of the water ligands. The axial and equatorial Pu–O (Pu–Oax and Pu–Oeq) bond lengths and coordination numbers are 1.7(2) O at 1.74(1) Å (Pu(VI)), 2.0(4) O at 1.82(1) Å (Pu(V)) and 3.7(4) O at 2.39(1) Å (Pu(VI)), 2.7(3) O at 2.50(1) Å (Pu(V)) (Table S2, ESI†).[9] We also optimized the structures of Pu(III)aq–Pu(VI)aq with the TURBOMOLE package (DFT/BP86 with TZVP basis sets) and obtained in most cases Pu–O bond lengths 0.038–0.185 Å longer compared to the EXAFS result (*cf.* Table S2, ESI†); one exception is Pu(V), with theoretical Pu–Oax and Pu–Oeq distances −0.082 and −0.033 shorter, respectively. These structures are used for calculation of Pu L_3 HR-XANES/DOS.

The Vis-NIR spectra of the Pu colloidal samples exhibit similar shapes (Fig. S2, ESI†); some show small (<4%) contributions of Pu(IV)aq and/or Pu(VI)aq. The intensity and the position of the characteristic peak at about 635 nm indicate Pu colloids of at least a few nm size as expected for "aged colloids" with equilibration time of 10 days–22 months (Table S1, ESI†).[5] TEM reveals an average size of 2–3 nm for the 9 months aged Pu colloids (*cf.* Fig. S3 and S4, ESI†). The structural parameters obtained from the EXAFS analyses of the Pu(IV)col samples are similar to crystalline PuO_2 with a face centred cubic (fcc) structure. Pu is bound to 7.9(1) O atoms at 2.30(1) Å. The second coordination sphere is modelled by 6.2(9) Pu atoms at 3.78(2) Å (Table S2 and Fig. S6, ESI†). The lower number of Pu atoms compared to stoichiometric bulk PuO_2 (8 O at 2.34 Å, 12 Pu at 3.82 Å, ICSD 55456) result from disorder in the colloids and or/their small size.[4,10] These results show 0.037(2) Å shortening of both Pu–O and Pu–Pu neighbour distances for the Pu(IV)col sample compared to bulk PuO_2 corresponding to a lattice constant a = 5.35 Å for Pu(IV)col in contrast to a = 5.398 Å for crystalline PuO_2 (Fig. S8, ESI†). An EXAFS study comparing fresh with aged Pu colloids reports a similar decrease of Pu–O and Pu–Pu distances, which is interpreted as partial Pu oxidation.[10] Rothe *et al.* report, however, an elongation for both Pu–O and Pu–Pu distances for freshly prepared colloidal Pu(IV),[4] whereas Hudry *et al.*[8] observe shortening only for Pu–O for synthetically prepared PuO_2 nanoparticles with 2–3 nm size. Obviously, structural variations typically depend on preparation, aging, particle size and the resulting level of atomic disorder.

The Pu L_3 and M_5 conventional XANES and HR-XANES spectra are depicted in Fig. 1a (L_3), Fig. 1c (M_5) and Fig. 1b (L_3), Fig. 1d (M_5), respectively. The WLs (peak A) have higher intensities for all HR-XANES spectra compared to the conventional XANES. The valence electronic configurations of Pu(III)–Pu(VI) are $5f^5 6d^0 7s^0$–$5f^2 6d^0 7s^0$. The L_3 and M_5 HR-XANES describe high probability electronic transitions of $2p_{3/2}$ electrons to Pu 6d/7s ($2p_{3/2} \rightarrow$ 6d/7s) and $3d_{5/2} \rightarrow$ 5f unoccupied states, respectively, governed by the dipole selection rule ($\Delta l \pm 1$, $\Delta s = 0$). The energy positions of the abrupt increase in absorption probability (absorption edge) are influenced by differences in the screening of the $2p_{3/2}$/$3d_{5/2}$ (and $3d_{5/2}$/$4f_{7/2}$ in fluorescence mode) core-holes by the electronic density on the Pu atoms and are used for Pu oxidation states analyses.[9] Caution is required in

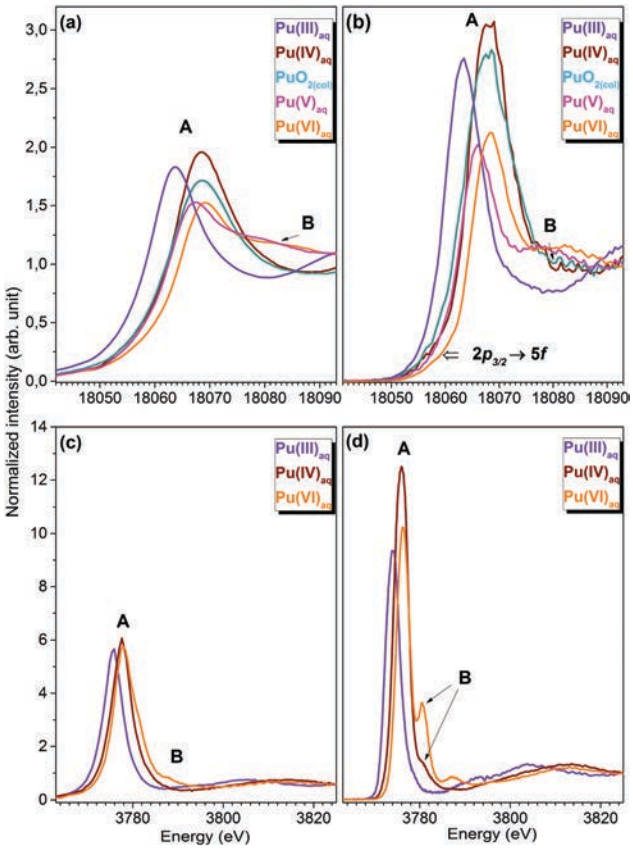

Fig. 1 Pu L_3 and M_5 XANES (a and c), L_3 and M_5 HR XANES (b and d) for Pu(III)aq Pu(VI)aq, Pu(IV)col (a and b) and for Pu(III)aq, Pu(IV)aq, Pu(VI)aq (c and d).

such analyses as covalency effects can influence the energy position of the absorption edge and the respective WL. One example where the energy position is shifted less than expected is the lower (−2.1 eV) and only slightly higher (+0.6 eV) Pu L_3 HR-XANES WL maxima energies for Pu(V)aq and Pu(VI)aq, respectively, relative to that for Pu(IV)aq (Fig. 1a and b). This is due to the accumulated electronic density in the vicinity of Pu as a result of the covalent Pu–Oax bond in plutonyl (Pu(V) and Pu(VI)).[9] The energy positions of the WLs (A) of the Pu L_3 HR-XANES spectra relative to Pu(III) in eV are: 18063.3(25) Pu(III)aq < +2.4(25) Pu(V)aq < +4.5(25) Pu(IV)aq + 9% Pu(VI)aq, Pu(IV)col < +5.1(25) Pu(VI); for the Pu M_5 edge HR-XANES: 3774.10(5) Pu(III)aq < +0.90(5) PuO_2 < +1.40(5) Pu(IV)col < +1.90(5) Pu(IV)aq + 6% Pu(VI)aq < +2.20(5) Pu(VI)aq. The Pu L_3 HR-XANES spectra of Pu(V)aq and Pu(VI)aq suggest the presence of a pre-edge feature with low intensity not visible in the conventional spectra (*cf.* Fig. S9, ESI†). Due to the high experimental energy resolution, it is possible to reveal weak $2p_{2/3} \rightarrow$ 5f quadrupole transitions appearing in the spectrum as for example discussed for U(VI)-yl.[11,12] If the inversion symmetry of the plutonyl molecule is destroyed the 5f will mix with 6d states and the intensity of this peak will increase due to the highly probable dipole transitions.[13] This can for example be an effective tool for detection of bending of the generally linear plutonyl molecule or asymmetric ligation in the equatorial or axial plane (*cf.* TOC). A pre-edge peak is

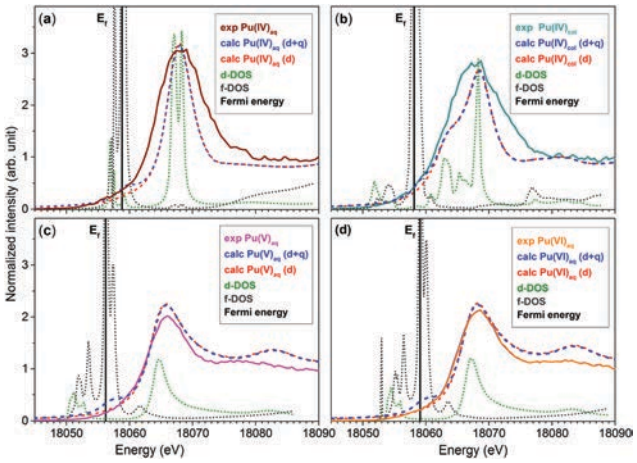

Fig. 2 Pu L_3 HR XANES: experiment and calculations with the FEFF9.5 code and Pu d and f DOS for Pu(IV)aq Pu(VI)aq and Pu(IV)col.

expected to be particularly evident for such cases involving Pu(VI) due to its having the highest number of f electron vacancies in the 5f shell and the anticipated associated increase in the energy separation between the 5f and the 6d states going from Pu(III) to Pu(VI). Results from quantum chemical calculations performed with the *ab initio* FEFF9.5 code substantiate this notion. The Pu d and f density of states (d-, f-DOS) are plotted along with the calculated and experimental Pu L_3 HR-XANES spectra in Fig. 2 (Fig. S11 ESI† for Pu(III)). As the dipole selection rule predicts, all spectra are described mainly by the unoccupied Pu d density of states (d-DOS); due to its diffuse nature, s-DOS has a broad, background like contribution (not shown). Evidence of participation of $2p_{2/3} \rightarrow 5f$ electronic transitions in the pre-edge region of the spectra appears in the spectra only by considering dipole ($2p_{2/3} \rightarrow 6d/7s$) and quadrupole ($2p_{2/3} \rightarrow 5f$) transitions in the calculations; no clear pre-edge is found when only dipole transitions are included.

The Pu L_3 HR-XANES experimental spectra for plutonyl also provide valuable geometric structural information. Peak B in Fig. 1 is typically associated with the multiple scattering of the Pu 2p photoelectron on the linearly arranged (O–Pu–O) Oax atoms;[9] The B and A resonances are better resolved in the HR-XANES compared to the conventional Pu L_3 HR-XANES spectra allowing for a more precise evaluation of the A–B energy separation (ΔE). ΔE has been previously correlated with the bond length (R) between Pu and the axial oxygen atoms (Oax): $\Delta E \cdot R^2$ = constant for *trans*-dioxo actinide An(VI)/An(V) bonds.[9] The energy shift between WL (A) and post-edge feature (B) is by 1.7 eV smaller for Pu(V)aq (12.5 eV) compared to Pu(VI)aq (14.2 eV), which correlates well with the Pu–Oax bond distance decrease from 1.82 Å in Pu(V)aq to 1.74 Å in Pu(VI)aq. The average value for the constant is 42.2 (eV Å^2) determined by using our experimental values for ΔE and R. This value reproduces the Pu(V)/Pu(VI)–O bond lengths obtained from EXAFS analyses with an error of ± 0.02 Å (Pu(VI)–O = 1.72 Å, Pu(V)–O = 1.84 Å). The post-edge of the computed Pu(V)aq spectrum is shifted by 4.2 eV to higher energies compared to the experiment mainly due to the 0.08 Å shorter calculated Pu–Oax distance (1.74 Å, experiment: 1.82 Å).

As expected, Pu(IV) is the predominant oxidation state for the aged Pu colloids with fcc structure similar to PuO_2. It is apparent in Fig. 1 that there is no energy shift between the Pu L_3 XANES and HR-XANES spectra of Pu(IV)aq and Pu(IV)col. Note that about 9% Pu(VI)aq and 4% Pu(IV)aq were present in the Pu(IV)aq and Pu(IV)col samples, respectively. The WL is reduced in intensity and exhibits an asymmetric shape for the Pu(IV)col spectrum compared to the Pu(IV)aq spectrum. The structures of bulk PuO_2 and computed molecular Pu(IV) were used to calculate the Pu(IV)col and Pu(IV)aq spectra, respectively (*cf.* Fig. 2). The calculated d-DOS for Pu(IV)col has a well resolved multi peak structure with a large energy gap of about 5 eV between the main peaks induced by the cubic crystal field. The d-DOS of Pu(IV)aq also exhibits two peaks; however, the energy gap between them is about 1 eV, and they are better defined, typical for molecular species. These results provide theoretical and experimental evidence for a condensation effects leading to band like Pu d states for the Pu(IV)col, instead of molecular d states in the aquo species. Our data also suggest cubic field splitting of the Pu d states, which corroborates the EXAFS results. Fig. 3 depicts the Pu M_5 edge HR-XANES spectra of the crystalline PuO_2, the Pu(IV)col and the 94% Pu(IV)aq + 6% Pu(VI)aq samples. Note that the PuO_2 solid sample is not diluted (*e.g.* with BN/cellulose); as a result, self-absorption leads to damping of the intensity of the main peaks. The Pu(IV)aq spectrum containing 6% of Pu(VI) shifts +0.5 and +1 eV to higher energies compared to the Pu(IV)col and the bulk PuO_2 spectra, respectively. In addition, a small peak at the energy position of 3781.04 eV, characteristic for peak B of Pu(VI) (arrow in Fig. 1d, inset in Fig. 3) is noticeable. This peak describes $3d_{5/2} \rightarrow 5f\sigma^*$ electronic transitions.[7] Pu M_5 HR-XANES is sensitive to small variations in Pu oxidation states and can detect 6% Pu(VI)aq present in Pu(IV)aq not possible with conventional XANES at the Pu L_3 and M_5 edges. The Pu M_5 HR-XANES for the Pu(IV)col does not exhibit shoulder B indicating that Pu(VI) is not present. Peak A is also shifted by +0.5 eV to higher energies compared to the spectrum of bulk PuO_2. Two of the

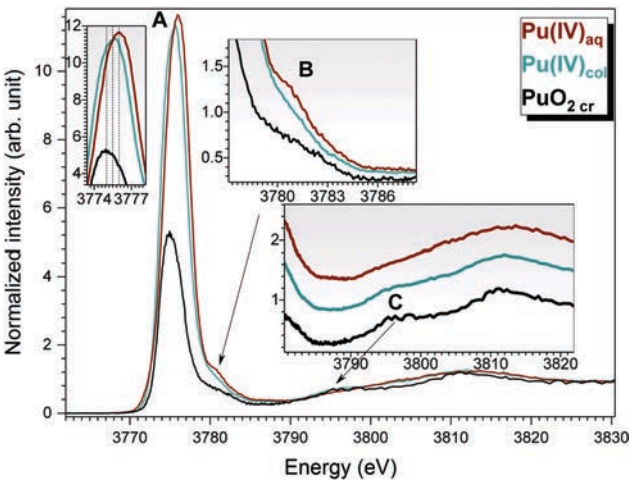

Fig. 3 Pu M_5 HR XANES for Pu(IV)aq containing 6% Pu(VI), Pu(IV)col and crystalline PuO_2.

plausible reasons for this +0.5 eV shift are related to the small size of the colloids and associated relative large surface to bulk ratio. Taking into account that the Pu colloids have cubic structure similar to PuO_2, it is possible that this shift is a result of contribution of a minor amount of Pu oxidation states higher than IV to compensate for surface charge and/or presence of more ionic Pu–OH/Pu–H_2O bonds. Another reason might be that Pu atoms at the colloid surface have nearest neighbour O atom defects compensating for charge. This can result in Pu 5f unoccupied states, which overall differ from that of bulk Pu atoms. One important observation is that the post-edge region of the Pu M_5 HR-XANES spectrum for the Pu(IV)col closely resembles the spectrum of PuO_2 (inset in Fig. 3). We have observed similarities for the post-edge regions of UO_2 and U_4O_9 (*cf.* Fig. S10, ESI†).[7] The latter has the cubic structure of UO_2 but part of U(IV) is oxidized to U(V). It is not possible to distinguish between the two compounds based only on the post-edge regions of the spectra, *i.e.* differences in the WL region need to be resolved. The structure of the aged Pu colloids might be analogous, *i.e.*, the cubic structure of PuO_2 is preserved but some of the Pu(IV) might be oxidized to Pu(V). Future studies including the comparison with Pu(V) HR-XANES spectra, studies of Pu colloids with systematic size variation and applying even higher energy resolution, which we have recently achieved,[6] will help to verify this hypothesis. The post edge region of the Pu(IV)aq spectrum differs from the spectra of the Pu(IV)col and PuO_2. This is likely due to lack of constructive interference of Pu–Pu scattering paths over a range of Pu–Pu distances, resulting in a featureless post-edge region of the Pu(IV)aq spectrum, *i.e.* feature C in Fig. 3 is nearly missing. We observed a similar effects for Pu dispersed in borosilicate glass.[6]

Pu L_3 and M_5 XANES and HR-XANES spectra of Pu(III), Pu(IV), Pu(V) (only L_3), Pu(VI) in aqueous solution, colloidal Pu(IV) and crystalline PuO_2 (only HR-XANES M_5) have been measured and the HR-XANES spectra have reduced spectral broadening resulting in better energy resolved features. We showed that this enhanced resolution allows using the Pu L_3 HR-XANES spectra for the estimation of An(V)/An(VI)–Oax bond lengths for actinyl cations and proposed that $\Delta E{\cdot}R^2 = 42.2$ (eV Å^2). This can be a valuable tool for studies of systems with Pu concentrations below the limit for EXAFS measurements. Our experimental results corroborated by theory, give evidence that the Pu 6d states condense and are split by the cubic crystal field when going from molecular to colloidal Pu(IV) species. This appears to be the main reason for reduction of the main peak intensity of the Pu L_3 edge XANES/HR-XANES spectra. Presence of Pu(V)/Pu(VI) oxidation states (plutonate), Pu–OH/Pu–OH_2 bonds and/or O vacancies onto the surface of the particles might also have contributions and this needs to be further investigated. The HR-XANES spectra measure relative energies within Pu 5f (M_5) and 6d (L_3) as well as between Pu 5f and 6d (L_3 edge) unoccupied valence states. This information can help to benchmark and drive improvement in theoretical approaches for calculations of Pu electronic structures.[7] The Pu M_5 HR-XANES technique is valuable for speciation investigations as it provides increased sensitivity to minor contributions of Pu oxidation states in samples containing mixtures, compared to Pu L_3 edge HR-XANES. For example, we could detect 6% Pu(VI) in Pu(IV)aq solution. Achieving even higher energy resolution is possible, so that the Pu M_5 HR-XANES might be potentially successful in detecting 2–4% Pu(V) present in the Pu colloids. The method can serve as an extremely valuable tool *e.g.* for the experimental verification of Pu(V) fractions existing in PuO_2 solids in presence of different oxygen levels and having a significant impact on Pu solubility as discussed in detail by Neck *et al.*[2,3]

Conflicts of interest

There are no conflicts to declare.

Notes and references

1 M. Altmaier, X. Gaona and T. Fanghanel, *Chem. Rev.*, 2013, **113**, 901 943.
2 C. Walther and M. A. Denecke, *Chem. Rev.*, 2013, **113**, 995 1015.
3 V. Neck, M. Altmaier and T. Fanghanel, *J. Alloys Compd.*, 2007, **444**, 464 469.
4 J. Rothe, C. Walther, M. A. Denecke and T. Fanghanel, *Inorg. Chem.*, 2004, **43**, 4708 4718.
5 C. Walther, J. Rothe, B. Brendebach, M. Fuss, M. Altmaier, C. M. Marquardt, S. Buechner, H. R. Cho, J. I. Yun and A. Seibert, *Radiochim. Acta*, 2009, **97**, 199 207.
6 S. Bahl, S. Peuge, I. Pidchenko, T. Pruessmarm, J. Rothe, K. Dardenne, J. Delrieu, D. Fellhauer, C. Jegou, H. Geckeis and T. Vitova, *Inorg. Chem.*, 2017, **56**, 13982 13990.
7 T. Vitova, I. Pidchenko, D. Fellhauer, P. S. Bagus, Y. Joly, T. Pruessmann, S. Bahl, E. Gonzalez Robles, J. Rothe, M. Altmaier, M. A. Denecke and H. Geckeis, *Nat. Commun.*, 2017, **8**, 1 9.
8 D. Hudry, C. Apostolidis, O. Walter, A. Janssen, D. Manara, J. C. Griveau, E. Colineau, T. Vitova, T. Prussmann, D. Wang, C. Kubel and D. Meyer, *Chem. Eur. J.*, 2014, **20**, 10431 10438.
9 S. D. Conradson, K. D. Abney, B. D. Begg, E. D. Brady, D. L. Clark, C. den Auwer, M. Ding, P. K. Dorhout, F. J. Espinosa Faller, P. L. Gordon, R. G. Haire, N. J. Hess, R. F. Hess, D. W. Keogh, G. H. Lander, A. J. Lupinetti, L. A. Morales, M. P. Neu, P. D. Palmer, P. Paviet Hartmann, S. D. Reilly, W. H. Runde, C. D. Tait, D. K. Veirs and F. Wastin, *Inorg. Chem.*, 2004, **43**, 116 131.
10 C. Ekberg, K. Larsson, G. Skarnemark, A. Odegaard Jensen and I. Persson, *Dalton Trans.*, 2013, **42**, 2035 2040.
11 T. Vitova, K. O. Kvashnina, G. Nocton, G. Sukharina, M. A. Denecke, S. M. Butorin, M. Mazzanti, R. Caciuffo, A. Soldatov, T. Behrends and H. Geckeis, *Phys. Rev. B: Condens. Matter Mater. Phys.*, 2010, **82**, 235118.
12 T. Vitova, J. C. Green, R. G. Denning, M. Loble, K. Kvashnina, J. J. Kas, K. Jorissen, J. J. Rehr, T. Malcherek and M. A. Denecke, *Inorg. Chem.*, 2015, **54**, 174 182.
13 T. Vitova, M. A. Denecke, J. Göttlicher, K. Jorissen, J. J. Kas, K. Kvashnina, T. Prüßmann, J. J. Rehr and J. Rothe, *J. Phys.: Conf. Ser.*, 2013, **430**, 012117.